

# PHASE CHANGE MATERIALS FOR THERMAL MANAGEMENT OF IC PACKAGES

DOC. ING. PAVEL FIALA, PHD.

ING. IVO BĚHUNEK, PHD.

ING. MILOSLAV STEINBAUER, PHD.

**Abstract:** This paper deals with the application of phase change materials (PCM) for thermal management of integrated circuits as a viable alternative to active forced convection cooling systems. The paper presents an analytical description and solution of heat transfer, melting and freezing process in 1D which is applied to inorganic crystalline salts. There are also results of numerical simulation of real 3D model. These results were obtained by means of the finite element method (FEM). Results of 3D numerical solutions were verified experimentally.

**Key words:** phase change, FEM, heat, integrated circuit

## INTRODUCTION

Phase change materials can store large amounts of heat without undergoing significant temperature changes because of their high latent heat of fusion. There are known the following basic PCM classification [9]

- 1) Inorganic  
Advantages – high latent heat, good thermal conductivity, non-flammable, cheap  
Disadvantages – corrosive effect on most metals, phase decomposition and loss of hydrate, supercooling.  
Examples –  $\text{CaCl}_2 \cdot 6\text{H}_2\text{O}$ ,  $\text{Na}_2\text{SO}_4 \cdot 10\text{H}_2\text{O}$  etc.
- 2) Organic  
Advantages – high latent heat, chemically stable, little or no supercooling, cheap, non-corrosive, non-toxic  
Disadvantages – low thermal conductivity, big volume changes during phase change, flammability  
Examples – paraffin wax, polyethyleneglycol, high-density polyethylene, stearic acid ( $\text{C}_{18}\text{H}_{36}\text{O}_2$ ), palmitic acid ( $\text{C}_{16}\text{H}_{32}\text{O}_2$ ) etc.
- 3) Compounds, combinations of amorphous and crystalline substances, clathrates etc.  
The amounts of stored energy are given by the calorimetric equation

$$Q = \rho V \Delta h_m + \int_{T_0}^{T_m} V \rho c dT + \int_{T_m}^{T_c} V \rho c dT \quad (1)$$

where  $\rho$  is the density,  $V$  the volume,  $c$  the specific heat,  $\Delta h_m$  the specific enthalpy,  $Q$  the heat,  $T_0$ ,  $T_m$ ,  $T_c$ , the initial, phase change and the final temperature of inorganic compounds during the accumulation process (see Fig. 1).

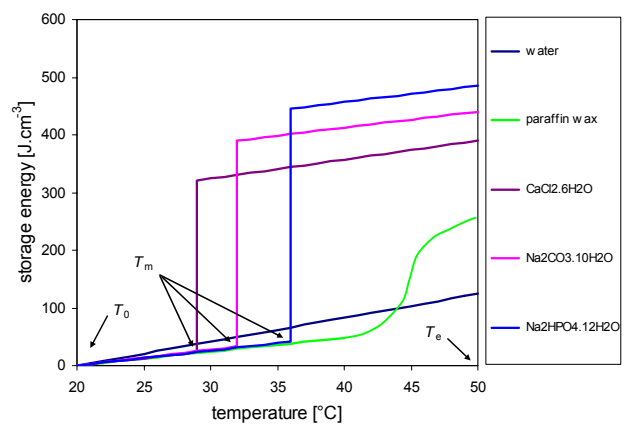
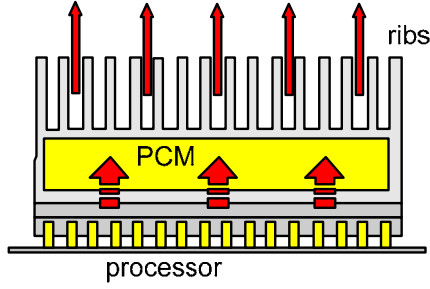


Fig. 1. Heating process of different PCMs and water (density of stored energy)

The PCM may be used for active or passive electronic cooling applications with high power at the package level (see [1]).



**Fig. 2.** Example of processor cooler with phase change material

## 1 ANALYTICAL DESCRIPTION AND SOLUTION OF HEAT TRANSFER AND PHASE CHANGE

We deal with the problem of heat transfer in 1D body during melting and freezing process with an external heat flux or heat convection, which is given by boundary conditions. The solution of this problem is known (Neumann, 1864) for solidification of metals [10]. We tried to apply this theory to melting of crystalline salts. The 1D body could be a semifinite plane, cylinder or sphere [3]. As the solid and the liquid part of PCM have different temperatures, there is a heat transfer on the interface. According to Fig. 3 the origin of  $x$  is the axis of pipe, centre of sphere or the origin of plate. Liquid starts to solidify if the surface is cooled by flowing fluid ( $T_w < T_m$ ).

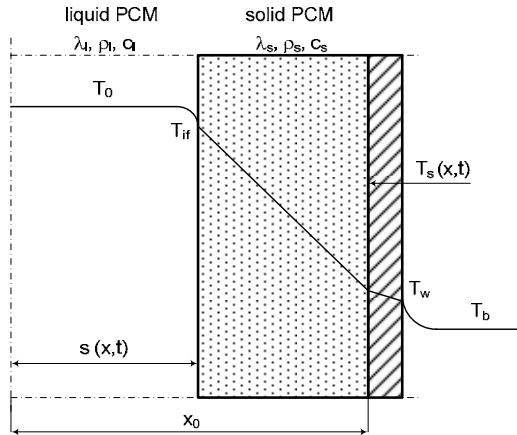


**Fig. 3.** Heat transfer on the interface between the solid and the liquid parts

The equation describing the solid state is

$$\frac{\partial T_s}{\partial t} = \frac{a_s}{x^n} \frac{\partial}{\partial x} \left( x^n \frac{\partial T_s}{\partial x} \right) \quad (2)$$

where for the plate  $n = 0$ , cylinder  $n = 1$  and sphere  $n = 2$ ,  $a_s$  is the thermal diffusion coefficient in the solid state. For  $x = x_0$  we can assume these boundary conditions

constant temperature

$$T = T_w \quad (3)$$

or constant heat flux

$$\lambda_s \frac{\partial T_s}{\partial x} = -q_w \quad (4)$$

or for convective cooling

$$\lambda_s = \frac{\partial T_s}{\partial x} = -k(T - T_b) \quad (5)$$

where  $q_w$  is the specific heat flux and  $\lambda_s$  is the thermal conductivity coefficient. Initial condition ( $t = 0$ ) for (2) is

$$T_s(0) = T_0. \quad (6)$$

For the interface between the solid and the liquid we obtain

$$\rho_s \Delta h_m \frac{ds}{dt} = \lambda_s \frac{\partial T_s}{\partial x} + \alpha(T_m - T_0). \quad (7)$$

The analytical solution is exact but we consider several simplifying assumptions. The most important of them is that we can solve the solidification of PCM only in one dimensional body.

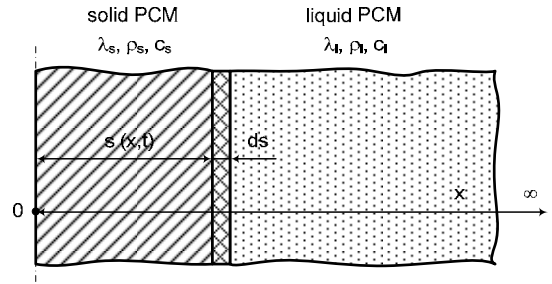


**Fig. 4.** Solidification of semi-infinite plate of PCM

We consider semi-infinite mass of liquid PCM at initial temperature  $T_0$  which has been cooled by a sudden drop of surface temperature  $T_p = 0$  °C. This temperature is constant during the whole process of solidification. The simplifying assumptions are

- body is semi-infinite plane
- heat flux is one-dimensional in the  $x$ -axis
- interface between the solid and the liquid is planar
- there is an ideal contact on the interface
- temperature of surface is constant ( $T_p = 0$  °C)
- crystallization of PCM is at a constant temperature  $T_m$
- thermophysical properties of the solid and the liquid are different but they do not depend on temperature
- there is no natural convection in the liquid.

Initial and boundary conditions:

- initial temperature  $T_0$  for  $x \geq 0$  at time 0
  - temperature equals  $T_m$  on the interface between the solid and the liquid ( $x = s$ )
- $$x = s \wedge t > 0 \Rightarrow T_s = T_l = T_m = const \quad (8)$$

- evolved latent heat during a motion of interface (the thickness of volume element  $ds$ , area  $1 \text{ m}^2$ , time  $1 \text{ s}$ )

$$dQ_{\Delta h_m} = \Delta h_m \rho_l 1 \frac{ds}{dt} \quad (9)$$

- position of interface is a function of time

$$s = s(t) = 2\varepsilon\sqrt{a_s t}, \quad (10)$$

this dependence is called the parabolic law of solidification, where  $\varepsilon$  is the root of equation describing the freezing.

- boundary and initial condition for phase change

$$\lambda_s \left( \frac{\partial T_s}{\partial x} \right)_{x=s} = \lambda_l \left( \frac{\partial T_l}{\partial x} \right)_{x=s} + \Delta h_m \rho_l \frac{ds}{dt} \quad (11)$$

$$x \rightarrow \infty \wedge t > 0 \Rightarrow T_l = T_0 = \text{const} \quad (12)$$

$$x = 0 \wedge t \geq 0 \Rightarrow T_p = T_s(x=0) = 0 \text{ } ^\circ\text{C} \quad (13)$$

If we solve the Fourier relations of heat conduction with conditions above for the solid and the liquid, we get the following equations which allow calculating temperatures in solid, liquid PCM and the location of interface. The results are in figures 5-8 which are related to equations 10, 15, 16.

$$\frac{e^{-\varepsilon^2}}{\text{erf}(\varepsilon)} \frac{\lambda_l}{\lambda_s} \sqrt{\frac{a_s}{a_l}} \frac{T_0 - T_m}{T_m} \frac{e^{-\frac{a_s \varepsilon^2}{a_l}}}{\text{erfc}\left(\varepsilon \sqrt{\frac{a_s}{a_l}}\right)} = \frac{\Delta h_m \rho_l \varepsilon a_s \sqrt{\pi}}{\lambda_s T_m} \quad (14)$$

We get  $\varepsilon = 0.3514$  for  $\text{CaCl}_2 \cdot 6\text{H}_2\text{O}$ ,  $\varepsilon = 0.3257$  for  $\text{Na}_2\text{CO}_3 \cdot 10\text{H}_2\text{O}$  and  $\varepsilon = 0.3319$  for  $\text{Na}_2\text{HPO}_4 \cdot 12\text{H}_2\text{O}$ .

$$T_s = \frac{T_m}{\text{erf}(\varepsilon)} \text{erf}\left(\frac{x}{2\sqrt{a_s t}}\right) \quad (15)$$

$$T_l = T_0 + \frac{T_0 - T_m}{\text{erfc}\left(\varepsilon \sqrt{\frac{a_s}{a_l}}\right)} \text{erf}\left(\frac{x}{2\sqrt{a_l t}}\right) \quad (16)$$

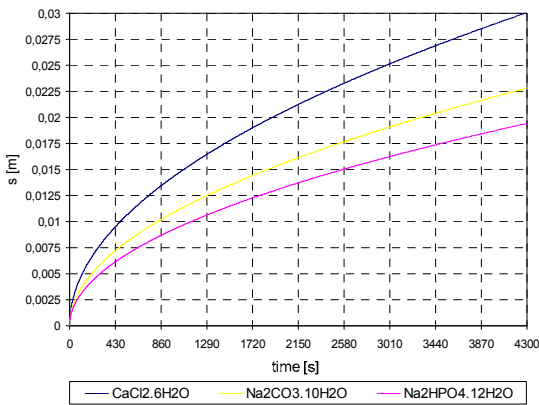


Fig. 5. Position between the solid and the liquid PCM

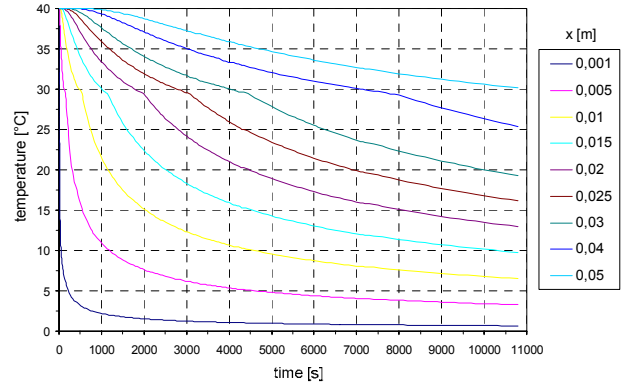


Fig. 6. Dependence of temperature on distance ( $\text{CaCl}_2 \cdot 6\text{H}_2\text{O}$ )

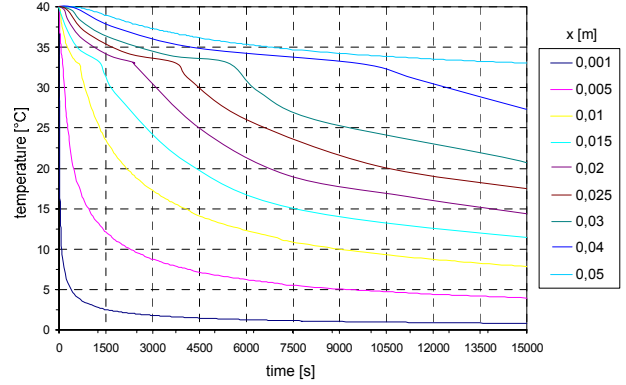


Fig. 7. Dependence of temp. on distance ( $\text{Na}_2\text{CO}_3 \cdot 10\text{H}_2\text{O}$ )

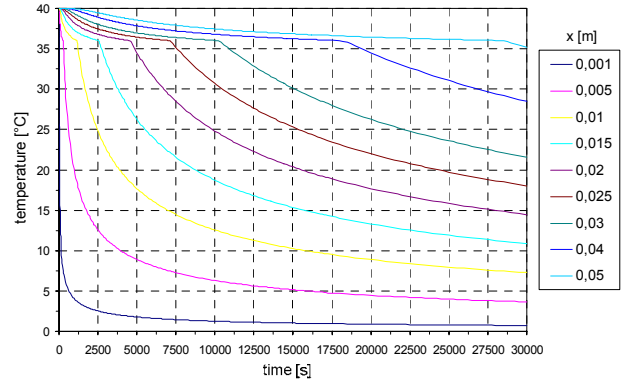


Fig. 8. Dependence of temp. on distance ( $\text{Na}_2\text{HPO}_4 \cdot 12\text{H}_2\text{O}$ )

If we compare results of the analytical solution with experimental measuring of those materials [4], we can see a good agreement.

## 2 MATHEMATICAL AND NUMERICAL MODEL

The thermal model is derived in detail in [6]. The mathematical model of air velocity distribution uses fluid equations which were derived for incompressible fluid with the condition (for the detailed description see [5])

$$\operatorname{div} \mathbf{v} = 0 \quad (17)$$

for a steady state of flow holds the continuity equation

$$\operatorname{div} \rho \mathbf{v} = 0 \quad (18)$$

We assume a turbulent flow

$$\operatorname{rot} \mathbf{v} = 2\boldsymbol{\omega} \quad (19)$$

where  $\boldsymbol{\omega}$  is the angular velocity of fluid. If we use the Stokes theorem, the Helmholtz theorem for moving particle and continuity equation, we can formulate from the equilibrium of forces the Navier-Stokes equation for the fluid element [11]

$$\frac{\partial \mathbf{v}}{\partial t} + (\operatorname{grad} \mathbf{v}) \cdot \mathbf{v}^T = \mathbf{A} - \frac{1}{\rho} \operatorname{grad} p + \mathbf{v} \cdot \Delta \mathbf{v} \quad (20)$$

where  $\mathbf{A}$  is the external acceleration and  $\mathbf{v}$  the vector of kinematic viscosity and  $(\operatorname{grad} \mathbf{v})$  has the dimension of tensor. In the equation (20) we substitute pressure losses

$$\begin{aligned} \operatorname{grad} p = & - \left( K_x \rho v_x |\mathbf{v}| + \frac{f}{D_h} \rho v_x |\mathbf{v}| + C_x \mu v_x \right) \mathbf{u}_x - \\ & - \left( K_y \rho v_y |\mathbf{v}| + \frac{f}{D_h} \rho v_y |\mathbf{v}| + C_y \mu v_y \right) \mathbf{u}_y - \\ & - \left( K_z \rho v_z |\mathbf{v}| + \frac{f}{D_h} \rho v_z |\mathbf{v}| + C_z \mu v_z \right) \mathbf{u}_z \end{aligned} \quad (21)$$

where  $K$  are the suppressed pressure losses,  $f$  the resistance coefficient,  $D_h$  the hydraulic diameter of ribs,  $C$  the air permeability of system,  $\mu$  the dynamic viscosity and  $\mathbf{u}$  the unit vector of the Cartesian coordinate system. The resistance coefficient is got from the Boussinesq theorem

$$f = a Re^{-b} \quad (22)$$

where  $Re$  is Reynolds number and  $a, b$  are coefficients from [14]. The model of short deformation field is formulated from condition of steady-state stability, which is expressed

$$\int_{\Omega} \mathbf{f} d\Omega + \int \mathbf{t} d\Gamma = 0 \quad (23)$$

where  $\mathbf{f}$  are the specific forces in domain  $\Omega$  and  $\mathbf{t}$  pressures, tensions and shear stresses on the interface area  $\Gamma$ . By means of the transformation into local coordinates we obtain the differential form for the static equilibrium

$$\mathbf{f} + \operatorname{div}^2 \mathbf{T}_v = 0 \quad (24)$$

where  $\operatorname{div}^2$  states for div operator of tensor quantity and  $\mathbf{T}_v$  is the tensor of internal tension

$$\mathbf{T}_v = \begin{bmatrix} X_x & X_y & X_z \\ Y_x & Y_y & Y_z \\ Z_x & Z_y & Z_z \end{bmatrix} \quad (25)$$

where  $X, Y, Z$  are the stress components which act on elements of area. It is possible to add a form of specific force from (17)-(20) to the condition of static equilibrium. The form of specific force is obtained by

means of an external acceleration  $\mathbf{A}$ , on condition that pressure losses and shear stresses  $\tau$  are given as

$$\rho \left( \frac{\partial \mathbf{v}}{\partial t} + (\operatorname{grad} \mathbf{v}) \cdot \mathbf{v}^T \right) - \rho \mathbf{A} - \sum_{l=1}^{N_s} \mathbf{F}_l + \operatorname{div}^2 \mathbf{T}_v = \mathbf{0} \quad (26)$$

where  $\mathbf{F}_l$  are the discrete forces and  $\operatorname{div}^2$  is the divergence operator of tensor. The model, which covers the forces, viscosity, and pressure losses is

$$\begin{aligned} \rho \left( \frac{\partial \mathbf{v}}{\partial t} + (\operatorname{grad} \mathbf{v}) \cdot \mathbf{v}^T \right) - \rho \mathbf{A} - \sum_{l=1}^{N_s} \mathbf{F}_l + \\ + \operatorname{grad} p - \mu \cdot \Delta \mathbf{v} = 0. \end{aligned} \quad (27)$$

We can prepare the discretization of equation (20) by means of the approximating of velocity  $\mathbf{v}$  and acceleration  $\mathbf{a}$

$$\begin{aligned} \mathbf{v} = \sum_{k=1}^{N_\phi} \mathbf{v}_{vk} W_k(x, y, z), \quad \forall (x, y, z) \in \Omega, \\ \mathbf{a} = \sum_{k=1}^{N_\phi} \mathbf{a}_{vk} W_k(x, y, z), \quad \forall (x, y, z) \in \Omega, \end{aligned} \quad (28)$$

where  $\mathbf{v}_v, \mathbf{a}_v$  are the instantaneous node values,  $W$  is the base function,  $N_\phi$  is the number of mesh nodes. If we apply the approximation (26) and the Galerkin principle in (27), we get the semidiscrete solution and after another rewriting we obtain the model of air flow

$$\begin{aligned} \rho \int_{\Omega} W_j W_i d\Omega \frac{d\mathbf{v}_{vi}}{dt} + \\ + \rho \int_{\Omega} W_j \mathbf{v}_{vi} \cdot \left( \frac{dW_i}{dx} \mathbf{u}_x + \dots + \frac{dW_i}{dz} \mathbf{u}_z \right) d\Omega \mathbf{v}_{vi} + \\ + \int_{\Omega} W_j \cdot \left( \frac{dW_i}{dx} \mathbf{u}_x + \dots + \frac{dW_i}{dz} \mathbf{u}_z \right) d\Omega p_i - \\ - \rho \int_{\Omega} W_j d\Omega \mathbf{A}_i - \int_{\Omega} W_j d\Omega \mathbf{F}_{li} - \\ - \int_{\Omega} \left( \frac{dW_j}{dx} + \frac{dW_j}{dy} + \frac{dW_j}{dz} \right) \mathbf{p}_i \cdot \\ \cdot \left( \frac{dW_i}{dx} \mathbf{u}_x + \frac{dW_i}{dy} \mathbf{u}_y + \frac{dW_i}{dz} \mathbf{u}_z \right) d\Omega \mathbf{v}_{vi} - \\ - \int_{\Gamma} W_j d\Gamma \mathbf{X}_i = 0, \quad i, j = 1, 2, \dots, N_v. \end{aligned} \quad (29)$$

On the interface there are boundary conditions formulated

$$\mathbf{n} \cdot (\mathbf{v}) = 0 \quad (30)$$

on the border  $\Gamma_{\text{air}}$  where  $\mathbf{n}$  is a normal vector to direction of air flow

$$\mathbf{n} \cdot (p) = 0 \quad (31)$$

on the border  $\Gamma_{\text{Cu}}$  where  $\Gamma_{\text{air}} \subset \Gamma_{\text{Cu}}$  is the interface between the solid body and air. Boundary conditions for thermal model are

$$\mathbf{n} \times (\operatorname{grad} T) = 0, \quad \text{on } \Gamma_{\text{air}} \cup \Gamma_{\text{PCM}} \quad (32)$$

and initial conditions

$$T(x, y, z, t)|_{t=0} = T_{0,\text{air}} = T_{0,\text{PCM}}, \quad \text{on } \Gamma_{\text{air}} \cup \Gamma_{\text{PCM}} \quad (33)$$

$$T(x, y, z, t)|_{t=0} = T_{0,\text{Cu}}, \quad \text{on } \Gamma_{\text{Cu}} \quad (34)$$

Initial conditions for the air flow in domain  $\Omega$  are

$$\mathbf{v}_{0,\text{air}}(z, t)|_{t=0} = 0, 1 \text{ m.s}^{-1}. \quad (35)$$

$$p_{0,\text{air}}(t)|_{t=0} = 10 \text{ Pa}. \quad (36)$$

out of domain  $W$  is the air velocity and pressure null.

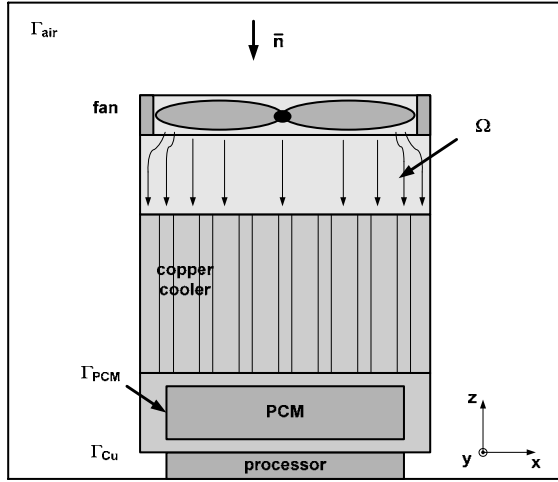


**Fig. 9.** Geometric model of Cu-cooler with mesh of elements

We can write the form for an element of mesh

$$\begin{aligned} [C_e^f] \left\{ \frac{d\mathbf{v}_{vi}}{dt} \right\} + [K_e^{sx} - K_e^{Fx}] \{\mathbf{v}_{vi}\} + [K_e^{cx}] p_i &= \\ = [K_e^{gx}] \{\mathbf{A}_i\} + [F_e^{bx}] \{\mathbf{F}_{li}\} + [F_e^{sx}] \{\mathbf{X}_i\} & \quad (37) \\ e = 1, 2, \dots, N_e. & \end{aligned}$$

Matrixes  $C_{ij}^f$ ,  $K_{ij}^{sx}$ ,  $K_{ij}^{Fx}$ ,  $K_{ij}^{cx}$ ,  $K_{ij}^{gx}$ ,  $F_{ij}^{bx}$ ,  $K_{ij}^{Fx}$ ,  $F_{ij}^{sx}$  are related to coefficients of equations (29).

For the solution we used the SST model (Shear Stress Transport Model) which is offered by the commercial software ANSYS FLOTTRAN. The SST model combines and switches between  $k-\varepsilon$  and  $k-\omega$  model automatically in order to get the best result (see [2], [7], [10]). The  $k-\varepsilon$  model gives good results in the distance from walls and  $k-\omega$  is more exact near walls. For the description of different turbulent models you can see [12], [13], [14].

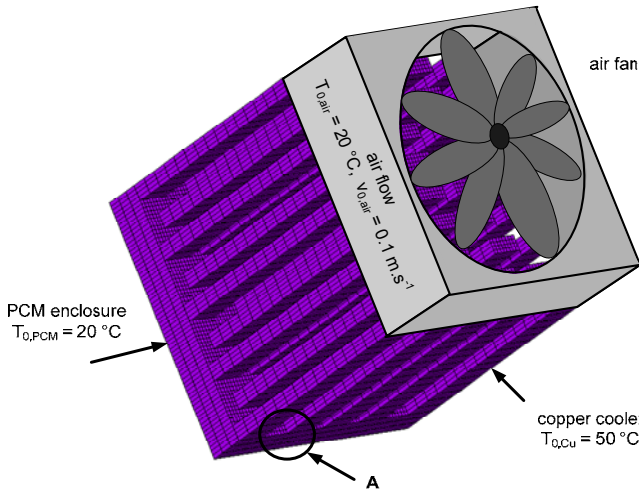


**Fig. 10.** Geometric model of Cu-cooler with mesh of elements

The progress of numerical solution consists of two parts. Firstly, we solve the turbulence model and get heat transfer coefficients on the surface of ribs. Those results are the input of second part when the thermal model is

calculated. We obtain the time dependence of temperature distribution in PCM. There is the geometric model of copper cooler in Fig.10. The  $\text{CaCl}_2 \cdot 6\text{H}_2\text{O}$  is closed inside of the bottom plate (see Fig. 2). The size of plate is  $30 \times 30 \times 5$  mm and ribs are 20 mm high. The PCM volume is about  $3,8 \cdot 10^{-6} \text{ m}^3$ . The plate takes heat from processor up and crystalline salt starts to melt at  $T_m$ . The air flows through ribs and extracts heat from the cooler.

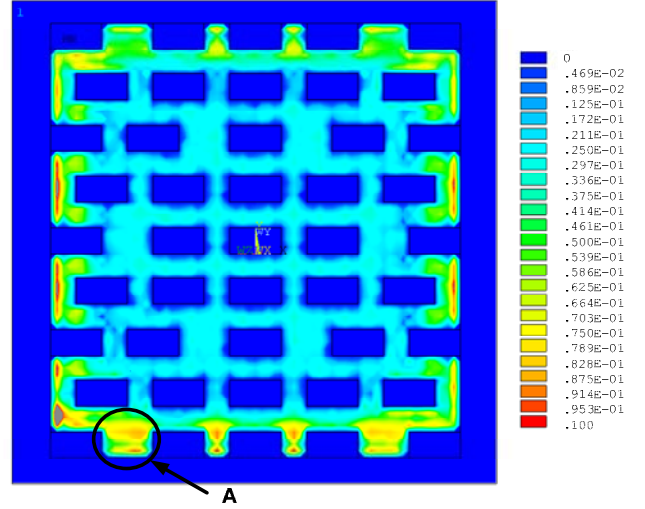


**Fig. 11.** The distribution of air velocity module

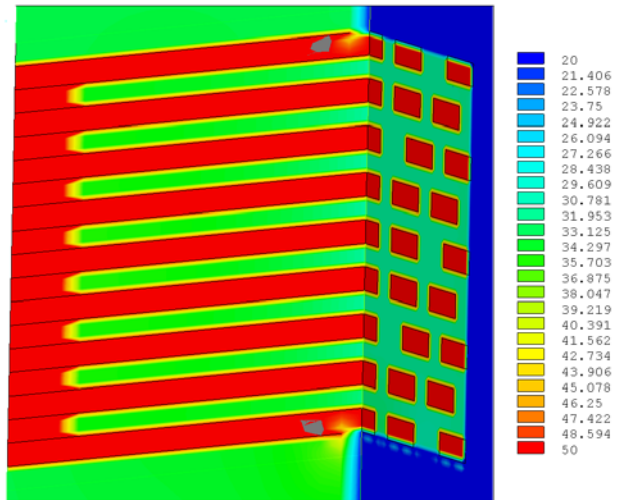


**Fig. 12.** Temperature distribution in the cooler (the cross section)

In Fig. 11 there is the distribution of air velocity module. We can see the effective rise of air flow velocity on the bottom of ribs (the detail A in Fig. 10, 11). Temperature distribution in ribs is shown in Fig 12. The Fig. 13 compares results of numerical simulation with the measuring in the middle of PCM enclosure. We measured the temperature by means of the probe. The differences between the simulation and the measuring are due to the inaccuracy of model with respect to reality. We used tabular values of pure  $\text{CaCl}_2 \cdot 6\text{H}_2\text{O}$  but we modified hexahydrate with 1,2% of  $\text{BaCO}_3$  in order to avoid supercooling and deformations of cooling curves after more cycles of melting and freezing. In order to obtain

exact results, we would need to know the temperature dependence of thermal conductivity, specific heat, and density during the phase change (see [8]).

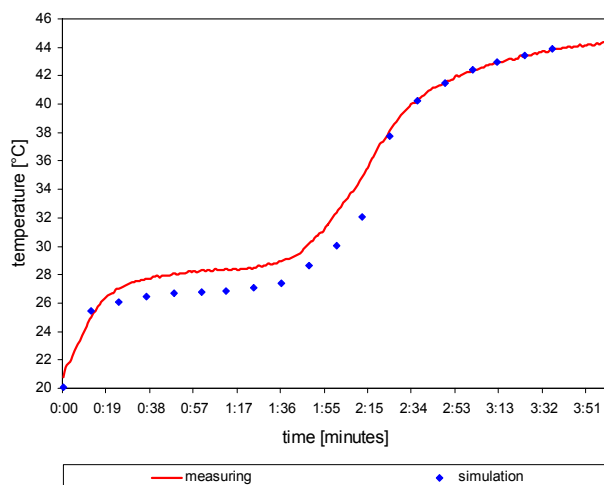


Fig. 13. Time dependence of temperature in  $\text{CaCl}_2 \cdot 6\text{H}_2\text{O}$

### 3 CONCLUSION

This paper dealt with the application of phase change materials for thermal management of integrated circuits. We presented analytical description and solution of heat transfer and phase change in 1D and also mathematical and numerical model of air turbulence. The model of real 3D copper cooler was solved by means of FEM in ANSYS software. We computed the problem of air flow turbulence, heat transfer, heat conduction and convection, and also phase change. If we compare results of simulation with the experimental measuring, we see good agreement. Exact knowledge of material properties has crucial effect on accuracy of numerical model.

### ACKNOWLEDGEMENTS

The paper was prepared within the framework of the research plan No. MSM 0021630516 of the Ministry of Education, Youth and Sports of the Czech Republic.

### 4 REFERENCES

[1] ADAM, J. Wärme- und Kühlmanagement in elektronischen Geräten. *Elektronik Praxis*. 2007, Vol. 3, Page 74-76.

[2] Ansys User's Manual. Huston (USA): SVANSON ANALYSYS SYSTEM, Inc., 1994-2006.

[3] ARSLANTÜRK, C. Small-time analytical solution of phase change problems in cylindrical and spherical domains. Turkey: *Journal of Thermal Sciences and Technology*. 2004.

[4] BĚHUNEK, I. Properties of inorganic PCM In Honeywell EMI conference and competition 2005. Brno: Ing. Zdeněk Novotný CSc., Ondráčkova 105, Brno, 2005. ISBN 80-214-2942-9.

[5] FIALA, P. Model indukčního průtokoměru DN-100 (výzkumná zpráva). UTEE FEKT VUT v Brně, Brno, 2001.

[6] FIALA, P. Modelování transformátoru při zkratu. PhD thesis. UTEE FEKT VUT v Brně, Brno, 1998.

[7] KOZEL, K. Numerické metody řešení problémů proudění I. Praha: Vydavatelství ČVUT.

[8] LAMBERG, P., LEHTINIEMI, R., HENELL, A-M. Numerical and experimental investigation of melting and freezing in phase change material storage. *Applied Mathematical Modelling* 32. 2004.

[9] LANE, G.A. Solar Heat Storage: Latent Heat Materials, Volume II: Technology. Boca Raton (Florida, USA): CRC Press, Inc., 1986.

[10] ŘÍHA, J. Matematické modelování hydrodynamických a disperzních jevů. Brno: Nakladatelství VUT., 1997. ISBN 80-214-0827-8.

[11] SPECHT, B. Modellierung von beheizten laminaren und turbulenten Strömungen in Kanälen beliebigen Querschnitts. Braunschweig (Germany): Technische Universität Carolo-Wilhelmina., 2000.

[12] PISZACHICH, W.S. Nonlinear Models of Flow, Diffusion and Turbulence. Leipzig (Germany): Teubner Verlagsgesellschaft, 1985.

[13] WILCOX, D.C. Turbulence modeling for CFD. La Canada (California, USA): DCW Industries, Inc., 1994.

[14] ZHANG, Y. Finite Elemente zur Berechnung instationärer Strömungen mit bewegten Wandungen. Stuttgart (Germany): Universität Stuttgart., 1996.

Brno University of Technology, Faculty of Electrical Engineering and Communication, Department of Theoretical and Experimental Electrical Engineering, Kolejní 2906/4, 612 00 Brno

Doc.Ing.Pavel Fiala, PhD., fialap@feec.vutbr.cz,  
Ing. Miloslav Steinbauer, PhD., steinbau@feec.vutbr.cz  
Ing.Ivo Běhunek, PhD., behunek@feec.vutbr.cz